NISTIR 5698

The Estimation of Measurement Uncertainty of Small Circular Features Measured by CMMs

S. D. Phillips
B. Borchardt
W. T. Estler

U.S. DEPARTMENT OF COMMERCE
Technology Administration
National Institute of Standards
and Technology
Gaithersburg, MD 20899

NIST

NIST IR WORKFORM

Create item:

Call number: QC100 .U56 NO.XX 19--

Class scheme: AUTO

Descriptive cataloging:

090 QC100|b.U56 no. 19--

100 1

245 --

260 Gaithersburg, MD :|bNational Institute of Standards and Technology,|c19--.

300

440 0 NISTIR ;|v

500

504

650 0

700 10

740 01

Label:

NIST-PUB-R
QC
100
.U56
NO.XXXX
19--

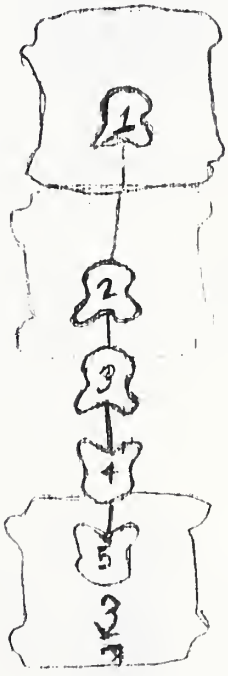

VI, 234 p. .11)

You have to come in late & Stay
late with me

I don't want to
Stay late by myself
today & Friday.

]

[710

NISTIR 5698

The Estimation of Measurement Uncertainty of Small Circular Features Measured by CMMs

S. D. Phillips
B. Borchardt
W. T. Estler

U.S. DEPARTMENT OF COMMERCE
Technology Administration
National Institute of Standards
and Technology
Gaithersburg, MD 20899

August 1995

U.S. DEPARTMENT OF COMMERCE
Ronald H. Brown, Secretary

TECHNOLOGY ADMINISTRATION
Mary L. Good, Under Secretary for Technology

NATIONAL INSTITUTE OF STANDARDS
AND TECHNOLOGY
Arati Prabhakar, Director

The Estimation of Measurement Uncertainty of Small Circular Features Measured by Coordinate Measuring Machines

S.D. Phillips, B. Borchardt, and W.T. Estler
Precision Engineering Division
National Institute of Standards and Technology

Abstract

This paper examines the measurement uncertainty of small circular features as a function of the sampling strategy, *i.e.,* the number and distribution of measurement points. Specifically, we examine measuring a circular feature using a three-point sampling strategy in which the angular distance between the points varies from widely spaced, 120 degrees, to closely grouped, a few degrees. Both theoretical and experimental results show that the measurement uncertainty is a strong function of the sampling strategy. The uncertainty is shown to vary by four orders of magnitude as a function of the angular distribution of the measurement points. A conceptual framework for theoretically estimating the measuring uncertainty is described and a good agreement with experiment is obtained when the measurements are consistent with the assumptions of the theoretical model.

Introduction

The determination of measurement uncertainty of coordinate measuring machines (CMMs) is a complex and daunting task. The very versatility that allows CMMs to inspect a wide range of features and part types makes evaluating the measurement uncertainty a multifaceted problem. Currently the vast majority of CMM measurements have no rigorous uncertainty budget. This is not to say that these measurements are significantly in error, but rather that their uncertainty is usually a guess based on the experience of the operator. While an experienced operator may often have a reasonable feeling for the capability of a CMM, there are measurement situations where intuition and experience may dramatically fail.

In this paper the evaluation of measurement uncertainty is described using the terminology and methodology recommended by the International Committee for Weights and Measures (CIPM) [1]. This terminology has been adopted by the International Organization for Standardization (ISO) and by national laboratories including NIST [2]. This methodology states that the uncertainty of a measurement result y can be quantified by the combined standard uncertainty u_c, given below. In this expression the measurand Y (the quantity being measured), is dependent on a number of different sources of uncertainty X_i (i = 1 to N).

$$Y = f(X_1, X_2, \ldots, X_N) \tag{1}$$

$$u_c^2 = \sum_{i=1}^{N} \left(\frac{\partial f}{\partial x_i} \right)^2 u^2(x_i) \quad + \quad 2 \sum_{i=1}^{N-1} \sum_{j=i+1}^{N} \frac{\partial f}{\partial x_i} \frac{\partial f}{\partial x_j} u(x_i, x_j) \tag{2}$$

This equation (loosely speaking) states that the combined uncertainty (characterized by its variance u_c^2) is the summation of each individual uncertainty source (characterized by its variance $u^2(x_i)$), multiplied by the square of a quantity known as the sensitivity coefficient (denoted $\partial f/\partial x_i$) whose magnitude describes the importance of the uncertainty source relative to the total measurement uncertainty. The quantity $u(x_i, x_j)$ is the covariance of x_i and x_j,and is a measure of the correlation between these two

uncertainty sources. The combined standard uncertainty, u_c, can be thought of as representing one standard deviation of the measurement uncertainty resulting from combining all known sources of uncertainties in the manner described by equation (2).

Although equation (2) describes the method of determining the combined standard uncertainty, the real work is in quantifying the sources of uncertainty by a variance, determining the correlation between these uncertainty sources, and in evaluating the sensitivity coefficients. Exactly how the measurement uncertainty sources are decomposed can depend on the specific measurement under investigation and the methods available to quantify the uncertainty sources. One general paradigm for separating CMM uncertainty sources is shown in Figure 1.

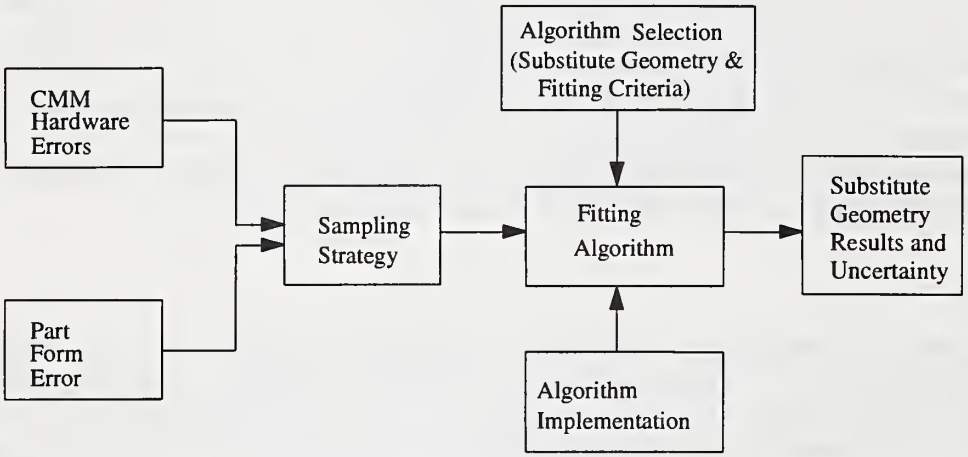

Figure 1. *Schematic outlining the various factors affecting CMM measurements.*

For the problem we are considering in this paper, namely the measurement of a small ring gauge, many of the issues shown in Figure 1 can be neglected. For example, since the form error of the ring gauge is on the order of 0.2 μm, the part form error is insignificant with respect to other sources of error. Furthermore, since the sampling strategy used involves only three points, the algorithm selection and implementation issues are rendered moot since three points exactly determine a circle and the problem becomes analytic. (However, tests were performed to ensure that other errors, such as the internal representation of numbers resulting in round off error, were insignificant.) Consequently, determining the combined standard uncertainty in our ring gauge measurements reduces to one of evaluating the uncertainty in the CMM and then determining the appropriate sensitivity coefficient for the particular sampling strategy used in the measurement. Since the aggregate of the CMM hardware errors manifest themselves as errors in the coordinates of the individual measurement points, conceptually the problem reduces to that shown in Figure 2.

Figure 2. *Schematic of the various factors affecting the CMM measurement of a small ring gauge.*

Experimental Estimation of Uncertainty

The measurement uncertainty of a small ring gauge (having a diameter of 47 mm (1.85 in)) can be estimated directly by repeated measurements in which parameters that are not strictly controlled during a normal part inspection are allowed to vary. (This is somewhat analogous to gauge repeatability and reproducibility studies in which factors such as changing the CMM operator can result in increased measurement variation.) In order to focus the scope of our investigation, we have minimized extrinsic factors such as operator variation, by using a computer controlled CMM, precisely specifying the sampling strategy, and employing a nearly perfect ring gauge. We do, however, vary the orientation of the sampling strategy coordinate system with respect to the machine coordinate system as discussed below. The quantity of interest is the measurement variation (a direct indication of measurement uncertainty) of each specified three-point sampling strategy, where the sampling strategy is defined by specifying the angle θ shown in Figure 3.

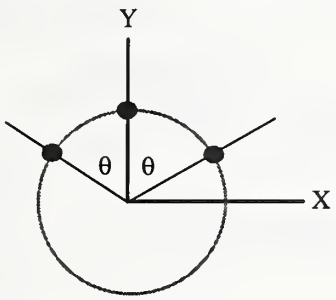

Figure 3. *Three-point sampling strategies which are defined by specifying the value of the angle* θ.

The measurement procedure is to define a coordinate system with the origin at the center of the ring gauge and the X and Y axes initially aligned along the machine coordinate system. The ring gauge is measured using the sampling strategy shown in Figure 3, *i.e.,* the three measurement points are symmetrically displaced with respect to the Y axis. The values of the radius and the X and Y circle center location are recorded. The coordinate system is then rotated about the origin by ten degrees with respect to the machine coordinate system, and the measurement repeated. This process is repeated a total of 36 times so that the sampling strategy and the defined coordinate system have been incremented in 10 degree steps around the entire ring gauge. Note that since the sampling strategy and defined coordinate system rotate together with respect to the machine coordinate system the sampling strategy is always identical to Figure 3, *i.e.,* the points are always symmetrically displaced with respect to the defined Y axis. Using the resulting 36 values of the ring gauge radius and center location, the standard deviation of each of these quantities is then computed. The entire process is repeated again for a different sampling strategy, *i.e.,* a different value of θ. The final result can be shown as a plot of the standard deviation of the fitted parameters (radius and center location) versus θ (which defines the sampling strategy), for example see Figure 4. Since different stylus lengths and probe types behave differently, the procedure was repeated for several common probe configurations as shown in Figures 4-8. Although a complete uncertainty analysis would include additional sources of uncertainty, *e.g.,* the thermal expansion of the gauge and the uncertainty in the effective stylus size, these factors can be accounted for in a straightforward manner. (These factors are independent of the sampling strategy and their uncertainty would be added in the usual (RSS) manner to the calculation of the combined standard uncertainty.)

It may seem unrealistic to inspect a ring gauge using points which are closely grouped together, however, there are many measurement situation where only a small partial arc of material is present which forces this situation. In such a partial arc case, it is clear that the uncertainty of the usual circle measurement is unexpectedly large and that an alternative may be needed such as fixing one of the circle parameters to its nominal value.

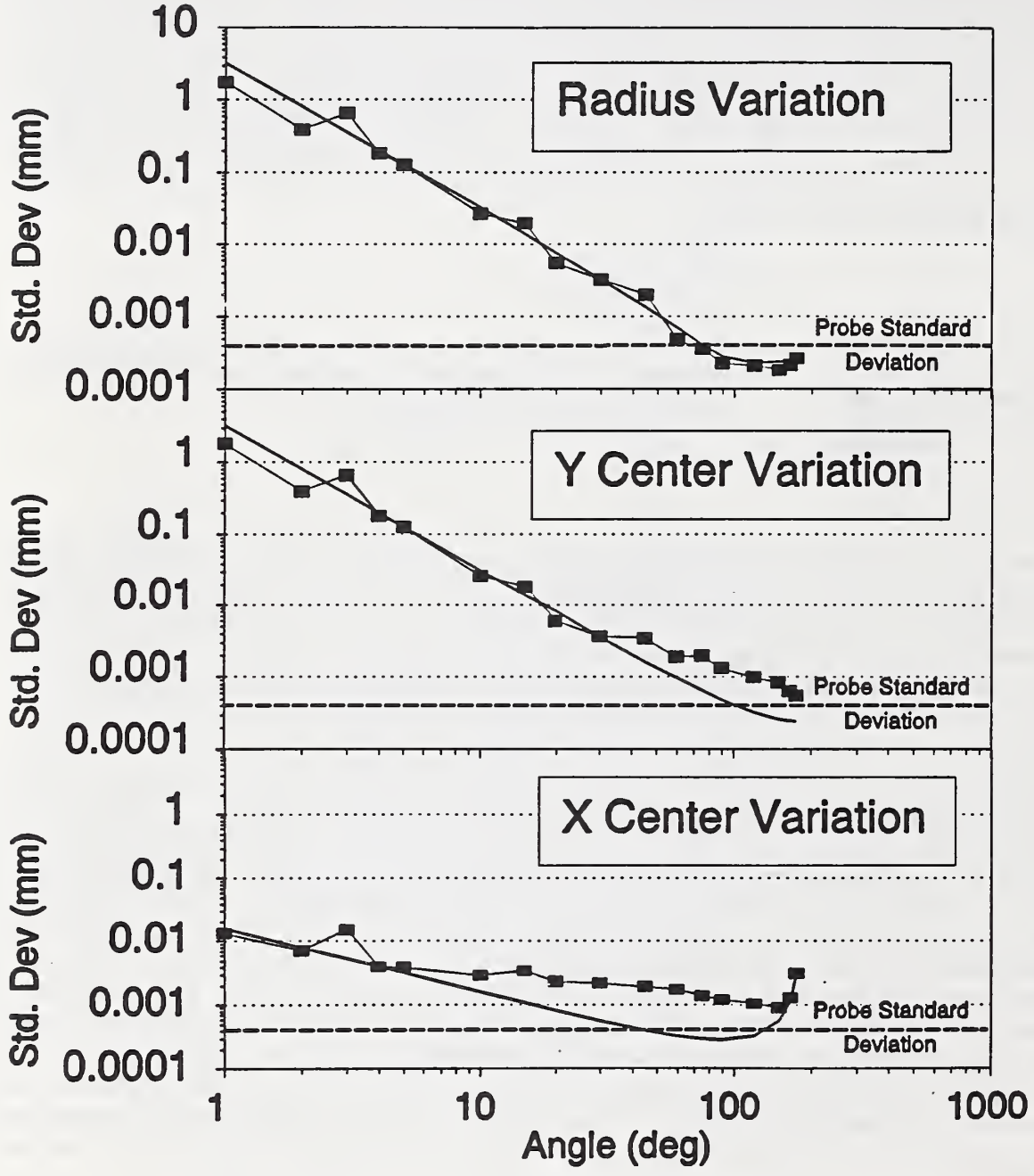

Figure 4. The standard deviation of radius and center location vs. sampling strategy angle for a TP 12 probe with a 50 mm long stylus.

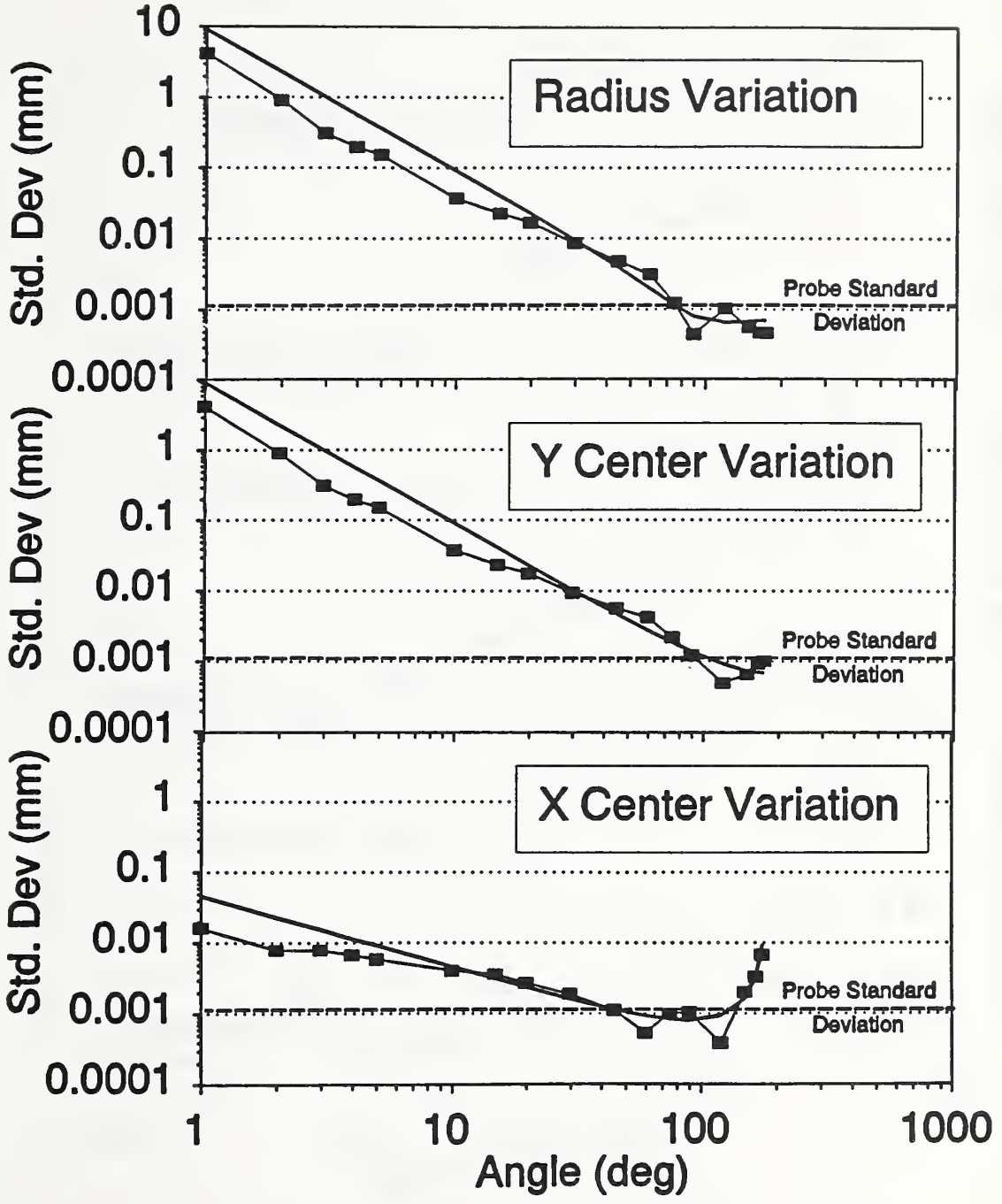

Figure 5. *The standard deviation of radius and center location vs. sampling strategy angle for a TP 6 probe with a 30 mm long stylus.*

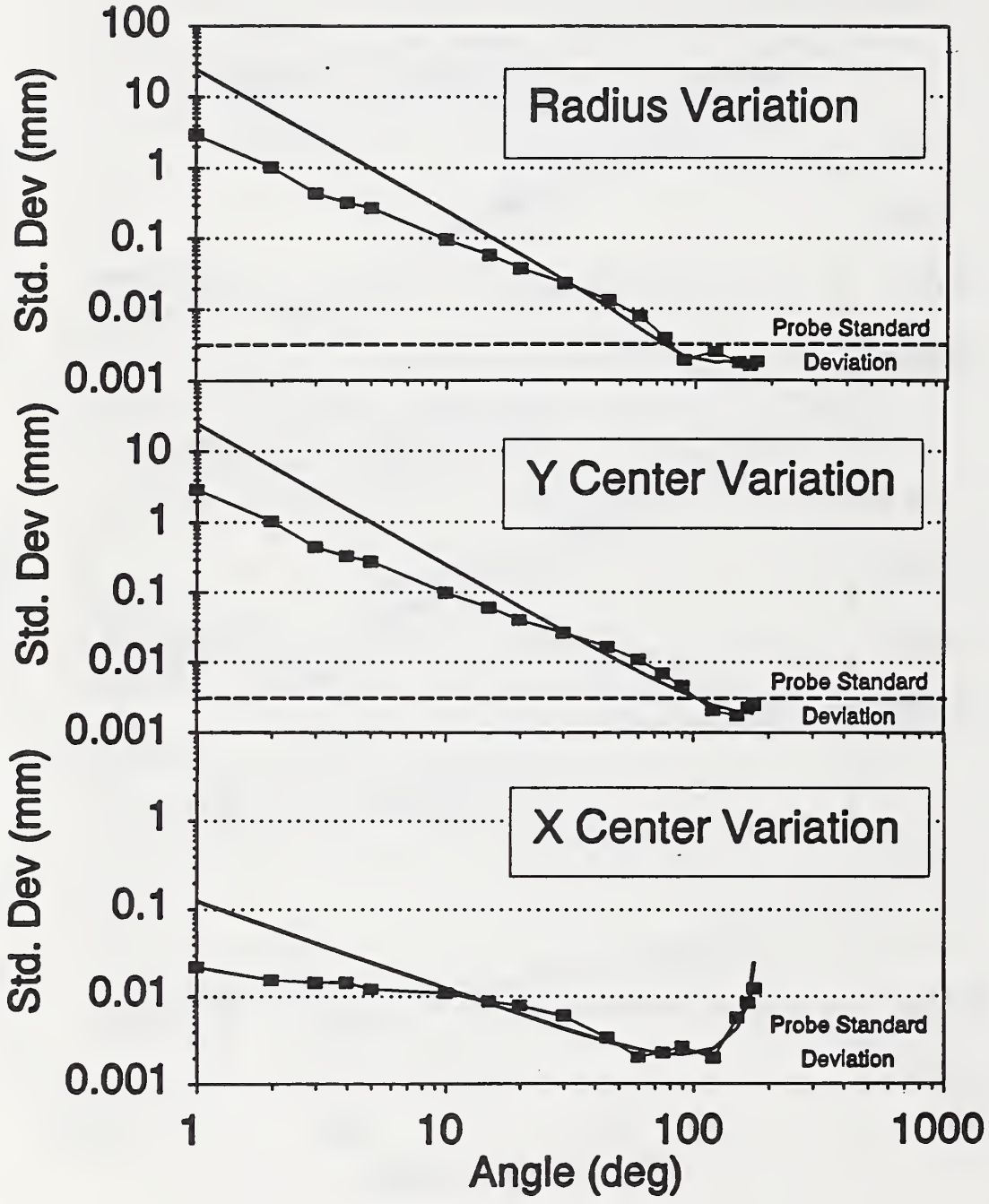

Figure 6. The standard deviation of radius and center location vs. sampling strategy angle for a TP 6 probe with a 50 mm long stylus.

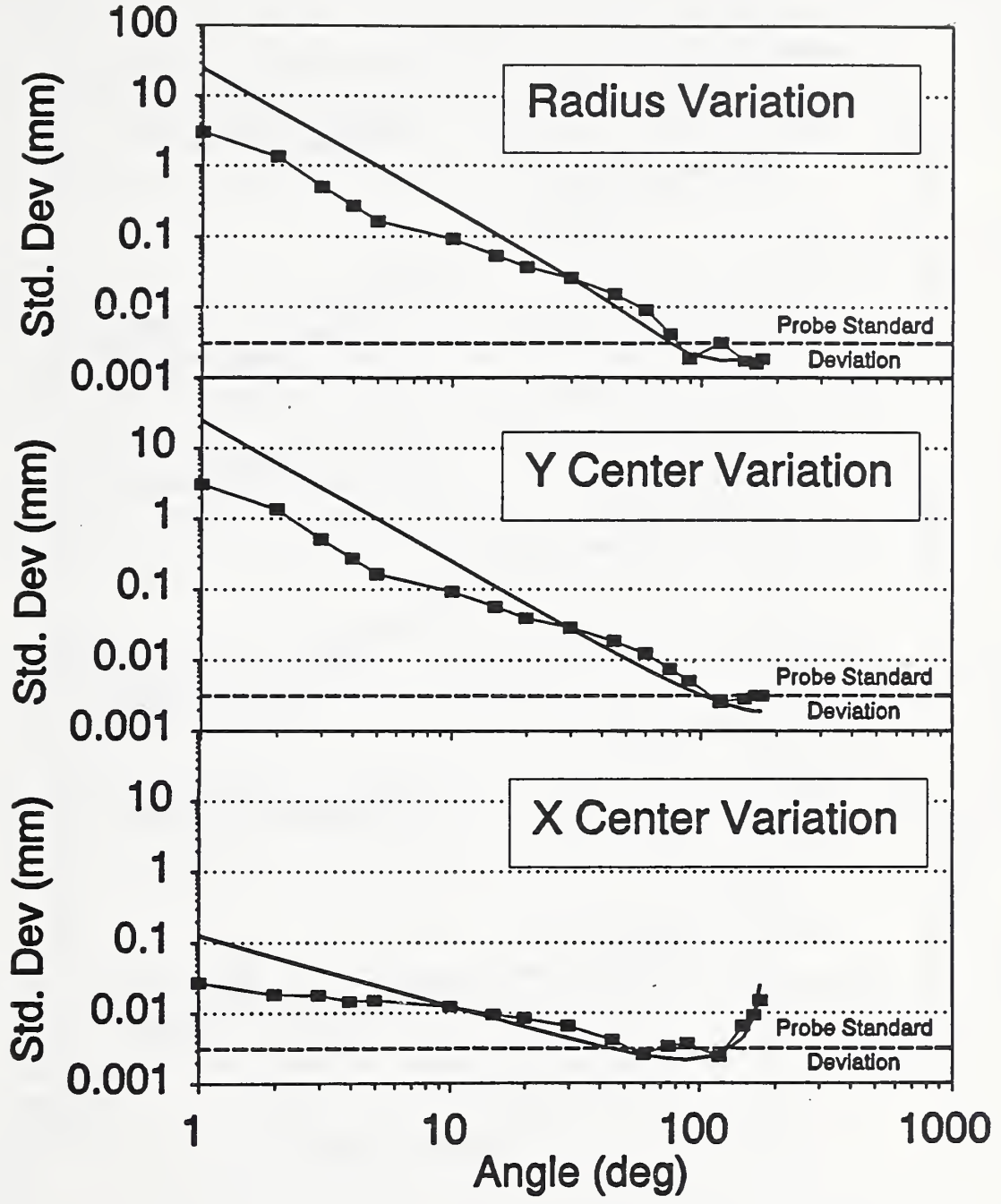

Figure 7. *The standard deviation of radius and center location vs. sampling strategy angle for a TP 2 probe with a 50 mm long stylus.*

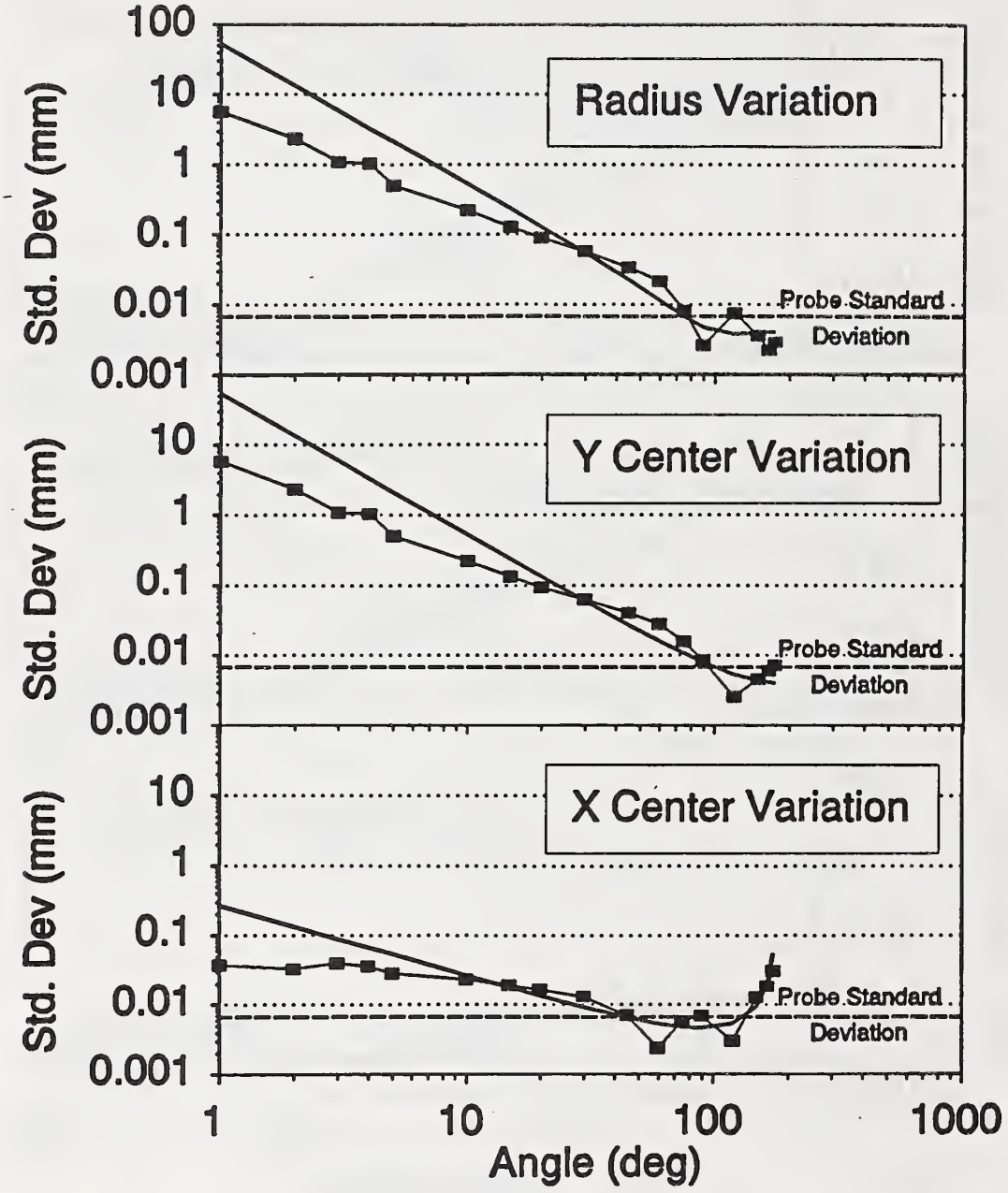

Figure 8. The standard deviation of radius and center location vs. sampling strategy angle for a TP 2 probe with a 100 mm long stylus.

Theoretical Estimates of Uncertainty

One benefit of a theoretical model of measurement uncertainty is to avoid the large number of measurements required to estimate the measurement uncertainty experimentally. Such measurements are both time consuming and costly, and may require a skilled metrologist to design the procedure. Using a theoretical model of the uncertainty allows the operator to determine the uncertainty directly, for example using a handbook, formula, or software program. Any theoretical model must contain two basic components, first an estimation of the uncertainty of the coordinates of each measurement point, and secondly a method to propagate the point coordinate uncertainty into the uncertainty of the substitute geometry, *e.g.,* the radius and center coordinates for the ring gauge.

A sophisticated model for determining the point coordinate uncertainty may include a detailed description of the machine. For example, all of the rigid body motion parameters (three translational and three rotational for each axis) may each have an associated uncertainty and their effects would propagate through to each measurement point. Similarly, other effects from causes such as nonrigid body behavior, hysteresis, thermally induced errors, and so forth, could also be included to describe the uncertainty of the CMM. Such a model would have a different value of uncertainty at each point in the CMM work zone, and in general, a different uncertainty for each coordinate (x, y, and z) at each point. The advantage of this approach is the ability to predict precisely the point coordinate uncertainty throughout the workzone. The disadvantage is the difficulty of developing a detailed model of the CMM and of the measurements needed to evaluate the model parameters. Additionally, the model parameters must be temporally stable or the predictions will degrade as the parameters drift from their assessed values. Additional aspects of estimating CMM measurement uncertainty can be found in [3].

For the measurement of a ring gauge, which is considered in this paper, most of the long range, *i.e.,* length dependent, sources of uncertainty can be neglected because the ring gauge has a very small diameter. For simplicity, we select a single parameter model of the CMM point coordinate uncertainty. This means that each point within the CMM workzone has the same uncertainty, and that these points are independent of one another, *i.e.,* their uncertainty is not correlated. Similarly, each coordinate (x, y, and z) of every point also has this same value of uncertainty. Obviously, using a single number to represent the uncertainty of the CMM is a tremendous over simplification; nevertheless in some cases the results can be surprisingly good. In the case of a machine with complete software error correction (including probe correction if the probe has significant lobing), the assumptions can be nearly true.

To estimate the value of this single parameter, which must be stated as a variance (or as a standard deviation) when using the CIPM formulation, we take the standard deviation of the radial residuals found from the ASME B89.1.12 probe performance test [4]. In this procedure 49 points are recorded on the surface of a small high precision sphere and a (least squares) best fit to a sphere is calculated. The radial residuals to each of the measurement points from the best fit radius are determined and their standard deviation is used for the single parameter to characterize the point coordinate uncertainty of the CMM. The sphere used in this measurement has a form error of less than 0.15 μm [5], and hence is negligible compared to the probe errors. Although this procedure is conducted on a small sphere, one can imagine its diameter shrinking to zero and the result being 49 measurements of the same (physical) point, with the standard deviation of these 49 values being characteristic of the uncertainty of the point. The advantage of this method is that most CMM users know about the B89 probe performance test and, hence, can easily perform the test to determine this value. As previously mentioned, such a simple model of the CMM will not accurately predict the uncertainty for all possible CMM measurements.

For the special case of a circle measured using a three-point sampling strategy the problem is analytic and allows a direct calculation of the substitute geometry uncertainty assuming that the errors at each of

the three points are independent, *i.e.*, are not correlated [6]. Therefore we can write down directly the combined standard uncertainty for each of the substitute geometry parameters as shown in equation (3), where u^2_{B89} is the variance of the radial residuals found from the B89.1.12 probe performance test and +... indicates that other sources of uncertainty should be included in the combined standard uncertainty. However, we are not explicitly considering them in this paper.

$$\begin{aligned} &\text{Radius:} && u_c^2 = \frac{1+2\cos^2\theta}{2(1-\cos\theta)^2}\, u_{B89}^2 + \ldots \\ &\text{Y center:} && u_c^2 = \frac{3}{2(1-\cos\theta)^2}\, u_{B89}^2 + \ldots \\ &\text{X center:} && u_c^2 = \frac{1}{2\sin^2\theta}\, u_{B89}^2 + \ldots \end{aligned} \tag{3}$$

Results

We have performed both the experimental and theoretical determinations of measurement uncertainty using the methods described for the measurement of a small ring gauge. In order to examine the generality of the results we have repeated the procedure using several different touch trigger probes and stylus combinations. For each probe type we have determined the standard deviation based on the B89 probe performance test. To accurately estimate this standard deviation we have repeated the B89 probe test a total of 10 times and used the mean of the results as the characteristic value. Table 1 presents the B89 results for the five probe configurations used in our study [7].

Table 1

probe configuration	standard deviation of the 49 radial residuals found from the B89 probe performance test (mean of 10 tests)	standard deviation of the 10 standard deviations
piezoelectric (TP12) 50 mm stylus	0.40 μm	0.03 μm
mechanical (TP 6) 30 mm stylus	1.14 μm	0.06 μm
mechanical (TP 6) 50 mm stylus	3.08 μm	0.11 μm
mechanical (TP 2) 50 mm stylus	3.10 μm	0.07 μm
mechanical (TP 2) 100 mm stylus	6.64 μm	0.15 μm

Figures 4-8 show both the experimental and theoretical determinations of the measurement uncertainty of the ring gauge as a function of sampling strategy for the probe configurations given in Table 1. The experimental results are the standard deviations of the 36 measurements of the ring gauge for each sampling strategy. The theoretical results are calculated using the values of Table 1 and the sampling strategy rules (which play the role of sensitivity coefficients) given in equation (3). The ordinate of these plots represents a single standard deviation. If an expanded uncertainty is required, then the uncertainty is increased by the coverage factor which is typically two, *i.e.*, twice the combined standard uncertainty. Also plotted for reference is the value of the B89 derived standard deviation shown in Table 1.

Discussion

The agreement between the experimentally determined standard deviation and that of the theoretically predicted standard deviation is reasonably good for all the probe configurations presented. It is clear that the sampling strategy plays an enormous role in the uncertainty. Neglecting this effect would lead to an uncertainty prediction that would be a constant for all values of θ, *i.e.,* would predict a straight line with a magnitude equal to the standard deviation found from the B89 probe performance test.

In the case of the piezoelectric probe the agreement between the experimental and theoretical results for the radial uncertainty is very good. We attribute this conformity to the fact that the piezoelectric probe is dominated by random (not systematic) errors and consequently the assumption implicit in the sampling strategy rules of independent uncorrelated errors at each measurement point is realized by this type of probe. The theoretical uncertainty tends to underestimate the variation in the X and Y center location by a small amount (on the order of one micrometer). We believe this is caused by thermal drift which is cumulative in the case of measuring the center location. This (and other) sources of uncertainty could have been added to the theoretical model but are not explicitly considered here because they are not the focus of this paper.

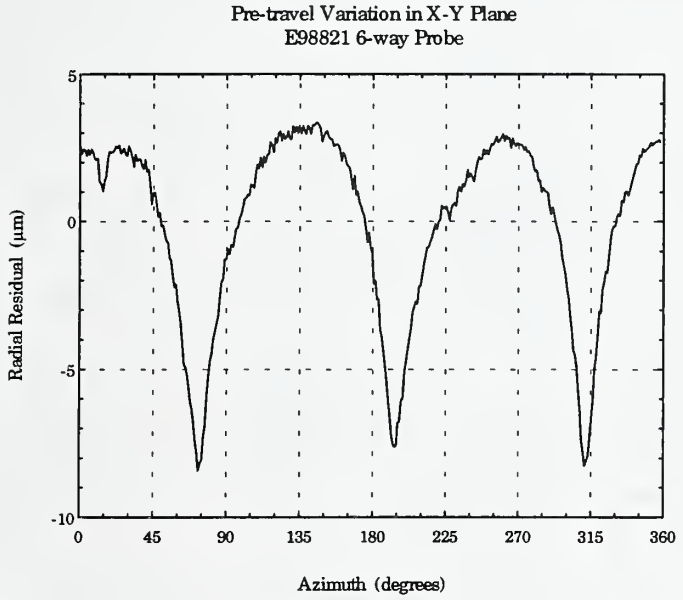

Figure 9.
The probe lobing of a mechanical touch trigger probe showing systematic probe errors

In the other touch trigger probes the mechanical structure supporting the stylus also serves as the electrical switch which is triggered when the stylus is displaced. This mechanism results in a directionally dependent sensitivity of the probe and is commonly called probe lobing because the measurement of circular parts with small form error appears to have a three-lobed shape, reflecting the triangular mechanical structure within the touch trigger probe. Figure 9 shows the three lobed pattern which is the result of this highly systematic error. For this class of probes the error at any measurement point is highly dependent upon the probe approach direction and hence for probe approach directions which are close together, the probing errors will be similar. Consequently, when θ is small, the three measurement points undergo the same perturbation, *i.e.,* have similar errors, and thus have significantly less variation between points than would be expected if the errors were truly independent as assumed in the theoretical model given by equation (3). Hence, the theoretically predicted variation is greater than that experimentally observed in the case of small θ. A more sophisticated model of the probe behavior which included this systematic effect [8] would be expected to improve the theoretically predicted uncertainty.

Summary

We have investigated the uncertainty of measuring a small ring gauge both experimentally and theoretically. Both methods show that the uncertainty can vary by four orders of magnitude, ranging from submicrometer to millimeters, depending upon the sampling strategy. Using a single parameter model to describe the CMM uncertainty, which is determined by the standard deviation of the radial residual of the B89 probe performance test, surprisingly good agreement between theory and experiment can be obtained. For touch trigger probes which exhibit systematic probe lobing the experimental results show less than the predicted variation when the measurement points are closely spaced because these points have correlated errors which reduces the variation in the fitted parameters of the substituted geometry.

Acknowledgments

This work was funded by NIST's computational metrology program, and by the Air Force's CCG program.

References

1. International Organization for Standardization, "Guide to the Expression of Uncertainty in Measurement," Geneva Switzerland, 1993.
2. B.N. Taylor and C.E. Kuyatt, "Guidelines for Evaluation and Expressing the Uncertainty of NIST Measurement Results," NIST Technical Note 1297, National Institute of Standards and Technology, Gaithersburg, MD 20899, 1993.
3. S.D. Phillips, "Chapter 7: Performance Evaluations," *Coordinate Measuring Machines and Systems*, edited by J. Bosch, Marcel Dekker Inc, 1995.
4. ANSI/ASME B89.1.12M (1990), "Methods for Performance Evaluation of Coordinate Measuring Machines," ASME, New York NY 1990.
5. G.W. Caskey, S.D. Phillips, B.R. Borchardt, D.E. Ward, and D.S. Sawyer, "A Users' Guide to NIST SRM 2084: CMM Probe Performance Standard," NIST Special Publication 260-120, National Institute of Standards and Technology, Gaithersburg, MD 20899, 1994.
6. T.H. Hopp, "The Sensitivity of Three-point Circle Fitting," NISTIR 5501, National Institute of Standards and Technology, Gaithersburg, MD 20899, 1994.
7. The identification of commercial products is given only for the sake of completely describing our experimental procedures. In no instance does such identification imply recommendation by the National Institute of Standards and Technology, nor does it imply that the particular equipment identified is necessarily the best available for the described purpose.
8. W.T. Estler, S.D. Phillips, B. Borchardt, T. Hopp, C. Witzgall, M. Levenson, K. Eberhardt, M. McClain, Y. Shen, and X. Zhang, "Error Compensation for CMM Touch Trigger Probes," to appear in the 1995 Proceedings of the American Society of Precision Engineering.